Correspondence to:
Professor W. Henderson,
Department of Chemistry,
University of Waikato,
Private Bag 3105,
Hamilton,
New Zealand
e-mail: w.henderson@waikato.ac.nz
FAX: 0064-7-838-4219

Tuning the sulfur-heterometal interaction in organolead(IV) complexes of $[Pt_2(\mu\text{-}S)_2(PPh_3)_4]$

Kristina Pham[a], William Henderson[a,*], Brian K. Nicholson[a] and T. S. Andy Hor[b,*]

[a]*Department of Chemistry, University of Waikato, Private Bag 3105, Hamilton, New Zealand*

[b]*Department of Chemistry, National University of Singapore, 3 Science Drive 3, Singapore 117543*

Received

Synopsis

Reactions of $[Pt_2(\mu\text{-}S)_2(PPh_3)_4]$ with Me_3PbOAc and Ph_2PbI_2 result in the formation of the cationic adducts $[Pt_2(\mu\text{-}S)_2(PPh_3)_4PbMe_3]^+$ and $[Pt_2(\mu\text{-}S)_2(PPh_3)_4PbPh_2I]^+$, which were found from X-ray structure determinations on their hexafluorophosphate salts to

contain four- and five-coordinate lead atoms, respectively. Fragmentation pathways of these and other related adducts are reported.

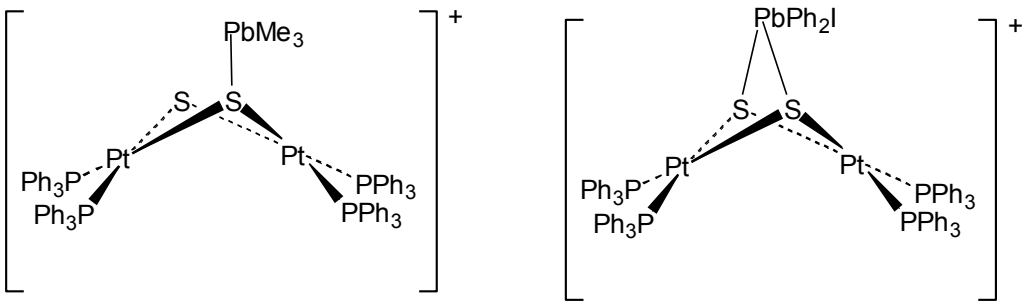

Abstract

Reactions of $[Pt_2(\mu\text{-}S)_2(PPh_3)_4]$ with Ph_3PbCl, Ph_2PbI_2, Ph_2PbBr_2 and Me_3PbOAc result in the formation of bright yellow to orange solutions containing the cations $[Pt_2(\mu\text{-}S)_2(PPh_3)_4PbR_3]^+$ (R_3 = Ph_3, Ph_2I, Ph_2Br, Me_3) isolated as PF_6^- or BPh_4^- salts. In the case of the Me_3Pb and Et_3Pb systems, a prolonged reaction time results in formation of the alkylated species $[Pt_2(\mu\text{-}S)(\mu\text{-}SR)(PPh_3)_4]^+$ (R = Me, Et). X-ray structure determinations on $[Pt_2(\mu\text{-}S)_2(PPh_3)_4PbMe_3]PF_6$ and $[Pt_2(\mu\text{-}S)_2(PPh_3)_4PbPh_2I]PF_6$ have been carried out, revealing different coordination modes. In the Me_3Pb complex, the (four-coordinate) lead atom binds to a single sulfur atom, while in the Ph_2PbI adduct coordination of both sulfurs results in a five-coordinate lead centre. These differences are related to the electron density on the lead centre, and indicate that the interaction of the heterometal centre with the $\{Pt_2S_2\}$ metalloligand core can be tuned by variation of the heteroatom substituents. The species $[Pt_2(\mu\text{-}S)_2(PPh_3)_4PbR_3]^+$ display differing fragmentation pathways in their ESI mass spectra, following initial loss of PPh_3 in all cases; for R = Ph,

loss of $PbPh_2$ occurs, yielding $[Pt_2(\mu\text{-}S)_2(PPh_3)_3Ph]^+$, while for R = Me, reductive elimination of ethane gives $[Pt_2(\mu\text{-}S)_2(PPh_3)_3PbMe]^+$, which is followed by loss of CH_4.

Keywords: Platinum complexes; Lead complexes; Sulfide ligands; Crystal structures; Electrospray mass spectrometry

Introduction

In a series of recent papers we have been applying the technique of electrospray ionisation mass spectrometry (ESI MS) to probe the coordination chemistry of the metalloligand $[Pt_2(\mu\text{-}S)_2(PPh_3)_4]$.[1,2,3,4] This methodology allows the rapid screening of reaction systems on a small scale, with promising systems then being investigated on a more traditional macroscopic scale for full characterisation.[5] Because the ESI technique involves soft ionisation, solution ions are transferred in an essentially intact state into the gas phase, so such an MS-directed synthetic methodology gives a good picture of solution speciation.

Using this methodology we have previously investigated organo-tin(IV) adducts of $[Pt_2(\mu\text{-}S)_2(PPh_3)_4]$[6] and of the related selenide complex $[Pt_2(\mu\text{-}Se)_2(PPh_3)_4]$[7], leading to the isolation and characterisation of a range of new Pt_2SnE_2 trimetallic aggregates. In this paper we report the extension of this methodology to adducts formed between $[Pt_2(\mu\text{-}S)_2(PPh_3)_4]$ and organo-lead(IV) compounds. To date, only adducts of (inorganic) lead(II) have been described; reaction of $[Pt_2(\mu\text{-}S)_2(PPh_3)_4]$ and $Pb(NO_3)_2$ gave $[Pt_2(\mu\text{-}S)_2(PPh_3)_4Pb(NO_3)_2]$ which with NH_4PF_6 gave $[Pt_2(\mu\text{-}S)_2(PPh_3)_4Pb(NO_3)]PF_6$, with both

complexes characterised by X-ray crystallography.[8] The related complex $[Pt_2(\mu\text{-}S)_2(dppf)_2]$ [dppf = 1,1'-bis(diphenylphosphino)ferrocene] forms a similar lead(II) adduct $[Pt_2(\mu\text{-}S)_2(dppf)_2Pb(NO_3)](NO_3)$[9] and lead(II) adducts of $[Pt_2(\mu\text{-}S)_2(PPh_3)_4]$ have been examined theoretically.[10]

Results

The reaction of $[Pt_2(\mu\text{-}S)_2(PPh_3)_4]$ with Ph_3PbCl in methanol rapidly led to the formation of a clear, bright yellow solution which was shown by ESI MS to contain solely the triphenyllead(IV) adduct $[Pt_2(\mu\text{-}S)_2(PPh_3)_4PbPh_3]^+$ (*m/z* 1941). From this solution, solid products **1a** and **1b** were readily isolable in good yields by addition of NH_4PF_6 or $NaBPh_4$ respectively. The complexes give satisfactory microanalytical data and are stable and soluble in polar solvents such as dichloromethane and chloroform. The cation could also be isolated as its $N(SO_2C_2F_5)_2^-$ salt **1c**, as orange-yellow crystals; the presence of the anion in this derivative was confirmed by negative-ion ESI MS. The reaction of $[Pt_2(\mu\text{-}S)_2(PPh_3)_4]$ with 0.5 mole equivalents of hexaphenyldilead ($Ph_3Pb\text{-}PbPh_3$) also results in the formation of $[Pt_2(\mu\text{-}S)_2(PPh_3)_4PbPh_3]^+$. Using this route, complex **1a** was isolated in 77% yield, and the product had identical ESI MS and $^{31}P\text{-}\{^1H\}$ NMR spectroscopic properties to **1a** prepared from Ph_3PbCl. The mechanism by which this reaction occurs is unknown, but $Ph_3Pb\text{-}PbPh_3$ has been well established as a source of Ph_3PbR compounds through Pb-Pb bond cleavage.[11] In contrast, no reaction was observed between $[Pt_2(\mu\text{-}S)_2(PPh_3)_4]$ and $PbPh_4$ in refluxing methanol.

The reaction of $[Pt_2(\mu\text{-}S)_2(PPh_3)_4]$ with Me_3PbOAc in methanol was more complex, and the products formed were dependent on the reaction time. A clear, bright yellow solution rapidly formed, and after a short reaction time (*ca.* 1 h), ESI MS showed the expected parent ion $[Pt_2(\mu\text{-}S)_2(PPh_3)_4PbMe_3]^+$ (*m/z* 1755) as essentially the sole species > *m/z* 400. A low intensity ion was observed at *m/z* 562, assigned to $[(Me_3Pb)_2OAc]^+$; this species has been observed previously in the ESI mass spectrum of Me_3PbOAc.[5] The trimethyllead adduct was isolated as its PF_6^- salt **2**, by addition of excess NH_4PF_6 to the filtered reaction solution; satisfactory microanalytical data were obtained. The ^1H NMR spectrum of the complex shows the $PbCH_3$ groups as a singlet at δ 1.16, showing coupling to ^{207}Pb of 61.5 Hz. This value can be compared to 68 and 63 Hz for Me_3PbBr and Me_3PbI respectively.[12] The $^{31}P\text{-}\{^1H\}$ NMR spectrum showed a single resonance at δ 23.2 with coupling to ^{195}Pt of 2944 Hz.

When the reaction between $[Pt_2(\mu\text{-}S)_2(PPh_3)_4]$ and Me_3PbOAc was monitored by ESI MS, $[Pt_2(\mu\text{-}S)_2(PPh_3)_4PbMe_3]^+$ was observed to form rapidly, followed by a much slower conversion to a species at *m/z* 1518, which was assigned to the mono-methylated species $[Pt_2(\mu\text{-}S)(\mu\text{-}SMe)(PPh_3)_4]^+$, confirmed by examination of the high resolution isotope pattern. This species is well-known from early studies on $[Pt_2(\mu\text{-}S)_2(PPh_3)_4]$; it has been synthesised from the reaction of $[Pt_2(\mu\text{-}S)_2(PPh_3)_4]$ with MeI in diethyl ether,[13,14] and has been generated *in situ* on a (MS-monitored) micro-scale by reaction of $[Pt_2(\mu\text{-}S)_2(PPh_3)_4]$ with a range of methylating agents, such as MeI, MeBr, Me_2SO_4, and $MeP(O)(OMe)_2$.[15] After 9 days, ESI MS of the reaction mixture showed predominantly $[Pt_2(\mu\text{-}S)(\mu\text{-}SMe)(PPh_3)_4]^+$, which was isolated as a crude hexafluorophosphate salt by addition of NH_4PF_6 to the filtered reaction mixture. The $^{31}P\text{-}\{^1H\}$ NMR spectrum of this

product showed two components. The first, $[Pt_2(\mu\text{-}S)(\mu\text{-}SMe)(PPh_3)_4]^+$, was easily identified by comparison of its spectral parameters with an authentic sample of $[Pt_2(\mu\text{-}S)(\mu\text{-}SMe)(PPh_3)_4]I$ prepared according to the literature procedure,[14] and found to have the same chemical shifts and $^1J(PtP)$ coupling constants as reported [2591 and 3220 Hz for phosphines *trans* to S and SMe respectively]. The second component gave a single ^{31}P resonance [δ 17.3, $^1J(PtP)$ 3101 Hz] indicating a symmetrical structure. The complex *cis*-$[Pt(SMe)_2(PPh_3)_2]$ can be ruled out on the basis of its reported ^{31}P NMR data [δ 25.5, $^1J(PtP)$ 2862 Hz],[16] but it is possible that the product is the *trans* isomer of $[Pt(SMe)_2(PPh_3)_2]$. The neutral complex $[Pt(SMe)_2(PPh_3)_2]$ would be expected to show a low ionisation efficiency in the ESI mass spectrum, however the mass spectrum of the crude product did show a very low intensity ion at *m/z* 766, assigned to $[Pt(SMe)(PPh_3)_2]^+$, an ion that might be expected to be observed for such a complex.

The reaction of $[Pt_2(\mu\text{-}S)_2(PPh_3)_4]$ with Et_3PbOAc was also investigated by ESI MS, and found to parallel that of the methyl system, giving the species $[Pt_2(\mu\text{-}S)_2(PPh_3)_4PbEt_3]^+$ at *m/z* 1797. However, conversion to the (previously unreported) ethylated derivative $[Pt_2(\mu\text{-}S)(\mu\text{-}SEt)(PPh_3)_4]^+$ at *m/z* 1532 occurred more rapidly. The relative reactivity of the methyl and ethyl systems was subsequently compared by the competitive reaction of $[Pt_2(\mu\text{-}S)_2(PPh_3)_4]$ with 0.5 molar equivalents of each of Me_3PbOAc and Et_3PbOAc in methanol. The starting materials quickly dissolved (< 1 minute) to produce a clear, bright yellow solution that contained equal amounts of $[Pt_2(\mu\text{-}S)_2(PPh_3)_4PbMe_3]^+$ and $[Pt_2(\mu\text{-}S)_2(PPh_3)_4PbEt_3]^+$ as the base peaks in the ESI mass spectrum. This was then followed by the slower conversion to the species $[Pt_2(\mu\text{-}S)(\mu\text{-}SR)(PPh_3)_4]^+$, with the ethyl derivative being formed significantly more rapidly.

Noteworthy in this reaction system was the observation of a (low intensity) species at *m/z* 1769, tentatively assigned to the mixed-alkyl species $[Pt_2(\mu\text{-}S)_2(PPh_3)_4PbMe_2Et]^+$, though interestingly $[Pt_2(\mu\text{-}S)_2(PPh_3)_4PbMeEt_2]^+$ was not observed.

The observation of the alkylated species $[Pt_2(\mu\text{-}S)(\mu\text{-}SR)(PPh_3)_4]^+$ (R = Me, Et) in reactions between $[Pt_2(\mu\text{-}S)_2(PPh_3)_4]$ and R_3PbOAc indicates that the R_3Pb^+ group is acting as an alkylating agent. Heavy element organometallics have previously been reported to act as alkylating or arylating agents,[17] including $PbMe_4$[18] and trimethyllead species.[19] In contrast, prolonged reaction (> 1 week) between $[Pt_2(\mu\text{-}S)_2(PPh_3)_4]$ and either Ph_3PbCl or Pb_2Ph_6 produced no phenylated derivative.

Diaryl-lead(IV) halide systems have also been investigated; the reaction of $[Pt_2(\mu\text{-}S)_2(PPh_3)_4]$ with Ph_2PbI_2 yielded an orange solution, containing predominantly $[Pt_2(\mu\text{-}S)_2(PPh_3)_4PbPh_2I]^+$ at *m/z* 1991 together with $[Pt_2(\mu\text{-}S)_2(PPh_3)_4PbPh_2]^{2+}$ at *m/z* 932. The dicationic nature of the latter ion was confirmed by its isotope distribution pattern. In this system, the soft iodide anion has a tendency to remain coordinated to the soft lead(IV) centre. On precipitation of the product with excess NH_4PF_6, an orange solid was obtained which gave good elemental microanalytical data for the iodo complex $[Pt_2(\mu\text{-}S)_2(PPh_3)_4PbPh_2I]PF_6$ **3**. The $^{31}P\text{-}\{^1H\}$ NMR spectrum showed a single sharp peak at δ 16.2, showing coupling to ^{195}Pt of 3068 Hz. However, the ESI MS spectrum (in methanol) of the isolated orange solid showed a roughly equal mixture of $[Pt_2(\mu\text{-}S)_2(PPh_3)_4PbPh_2I]^+$ and $[Pt_2(\mu\text{-}S)_2(PPh_3)_4PbPh_2]^{2+}$. It is feasible that in a polar solvent (such as methanol) some dissociation occurs due to the low concentration of iodide in the polar solvent. Consistent with this, addition of a small quantity of aqueous NaI solution to the methanol analyte solution resulted in complete conversion to the iodo complex

$[Pt_2(\mu\text{-}S)_2(PPh_3)_4PbPh_2I]^+$. Recrystallisation of the iodo complex **3** by vapour diffusion of diethyl ether into a dichloromethane solution gave a homogenous sample of orange blocks of the complex suitable for an X-ray diffraction study, which confirmed its formulation, as described in the following section. Analysis of one crystal by ESI MS again showed the iodo complex as the base peak, but with $[Pt_2(\mu\text{-}S)_2(PPh_3)_4PbPh_2]^{2+}$ still observed (50% relative intensity).

In a similar manner, reaction of $[Pt_2(\mu\text{-}S)_2(PPh_3)_4]$ with Ph_2PbBr_2 gave a yellow solution which furnished the analogous bromo complex $[Pt_2(\mu\text{-}S)_2(PPh_3)_4PbPh_2Br]PF_6$ **4** on addition of NH_4PF_6. This complex showed similar ^{31}P NMR spectroscopic parameters to the iodo complex [δ 16.1, ^1J(PtP) 3087 Hz], and also showed analogous behaviour in ESI MS analysis, giving both $[Pt_2(\mu\text{-}S)_2(PPh_3)_4PbPh_2Br]^+$ (*m/z* 1944) and $[Pt_2(\mu\text{-}S)_2(PPh_3)_4PbPh_2]^{2+}$ (*m/z* 932). Likewise, reaction of $[Pt_2(\mu\text{-}S)_2(PPh_3)_4]$ with Ph_2PbBr_2 followed by addition of a large excess of KSCN yielded a yellow solid which analysed as the thiocyanato derivative $[Pt_2(\mu\text{-}S)_2(PPh_3)_4PbPh_2SCN]SCN$ **5** on the basis of ESI MS (product cation at *m/z* 1922), $^{31}P\text{-}\{^1H\}$ NMR [δ 15.74, ^1J(PtP) 3091] and elemental analysis.

X-ray structure determinations on $[Pt_2(\mu\text{-}S)_2(PPh_3)_4PbMe_3]PF_6$ 2 and $[Pt_2(\mu\text{-}S)_2(PPh_3)_4PbPh_2I]PF_6$ 3

The structure of the cation of the trimethyllead derivative **2** is illustrated in Figure 1. It consists of the usual $P_4Pt_2S_2$ core with the Me_3Pb^+ group attached to one of the two S atoms. There is no significant interaction with the other S atom, as evidenced by the

longer Pb-S distance [3.835(1) Å c.f. 2.611(1) Å for the bonded one] and by the symmetrical geometry around the Pb atom (C-Pb-C angles essentially equal at 115.0±1.6°). For comparison, Me_3PbSMe has a Pb-S distance of 2.588 Å and C-Pb-C angles of 117±2°.[20] The Pt-S distances to the lead-bonded S atom average 2.374 Å, while those to the two-coordinate S are 2.329 Å. It is noteworthy that in the $^{31}P-\{^1H\}$ NMR spectrum of this complex, a single sharp resonance was observed at room temperature, suggesting that the complex is fluxional in solution, with the $PbMe_3$ group hopping between S centres. Upon cooling to 223 K, the spectrum remained essentially unchanged, suggesting a very facile exchange process.

In contrast, the structure of the Ph_2IPb^+ analogue **3** shown in Figure 2 has the lead atom interacting with both S atoms, though not equally. The Pb-S(1) distance is short at 2.567(2) Å, while Pb-S(2) is 2.879(2) Å. This results in a five-coordinate Pb atom with pseudo trigonal bipyramidal coordination, the I and S(2) atoms occupying the axial positions [I-Pb-S(2) angle 156.6°]. A similar arrangement was also found for the corresponding Me_2ClSn^+ and $(PhCH_2)_2BrSn^+$ analogues.[1] Related systems are known in the literature, for example the complex $[Ph_2Pb(dmit)]$ (H_2dmit = 4,5-dimercapto-1,3-dithiole-2-thione], which adds iodide to give $[Ph_2Pb(dmit)I]^-$; the same product is formed from Ph_2PbI_2 and $(Et_4N)_2[Zn(dmit)_2]$.[21]

The Pb-I distance of 2.9208 Å in **3** is longer than the equivalent in a four-coordinate R_3Pb-I compound (2.849 Å)[22] but is similar to a pseudo-five coordinate equivalent with an intramolecular coordinated $–NMe_2$ group (2.956 Å).[23] Presumably it would take little to remove the I atom and convert **3** into the dication $[Pt_2(\mu\text{-}S)_2(PPh_3)_4PbPh_2]^{2+}$ with a Ph_2Pb group symmetrically attached to both S atoms. This is

consistent with the observation that the 'parent' $[Pt_2(\mu\text{-}S)_2(PPh_3)_4PbPh_2I]^+$ cation readily loses iodide in ESI MS analysis, giving $[Pt_2(\mu\text{-}S)_2(PPh_3)_4PbPh_2]^{2+}$.

One significant difference between **2** and **3** is the dihedral angle formed by the two P_2PtS_2 planes in each cation, 138.1° for **2** and 126.3° for **3**. There are approximately 70 examples of derivatives of $(Ph_3P)_4Pt_2S_2$ in the Cambridge Crystallographic Database (May 2006 version), most of these having the equivalent dihedral angle in the range 123-147° with a mean value of 134° (excluding the parent complex with an angle of 168°,[24] and two unusual examples with two AuCl or AgCl groups attached to the S atoms, with angles of 180°.[25]) However there doesn't seem to be any particular pattern to variations in this fold-angle in terms of the number or type of groups attached to the sulfur atom(s), so it appears it is a flexible parameter determined by intra-molecular and crystal packing interactions and isn't a consequence in **2** and **3** of differing Pb coordination.

Electrospray mass spectrometry study

A study of the cone voltage-induced fragmentation of the organolead(IV) adducts $[Pt_2(\mu\text{-}S)_2(PPh_3)_4PbMe_3]^+$ and $[Pt_2(\mu\text{-}S)_2(PPh_3)_4PbPh_3]^+$ has been carried out, in order to explore differences in fragmentation pathways imposed by the different organic groups. A number of studies have previously concerned the ESI MS analysis of organolead complexes. In an early study, the ESI MS behaviour of Me_3PbCl and Et_3PbCl were studied and yielded the parent $[R_3Pb]^+$ cations under low fragmentation conditions.[26] At a fragmentor voltage of 100V, the most abundant fragment ions were formed by loss of R-R, while at 150V, the bare lead cation $[Pb]^+$ was observed. Similar results have been

observed for Me_3PbOAc.[5] Aryllead(IV) carboxylates have also been studied[27] and ESI has been used in the 'bare metal' or 'elemental' mode, for the quantitative analysis of organolead compounds.[28] A study of diphenyl lead(IV) thiosemicarbazonate complexes found that fragmentation by loss of two phenyl groups occurred first, giving product ions in which the Pb-S bond is retained.[29]

Positive-ion ESI mass spectra for $[Pt_2(\mu\text{-}S)_2(PPh_3)_4PbPh_3]PF_6$ **1a** in dichloromethane-methanol solution are shown in Figure 3. At low cone voltages, e.g. up to 50 V (Figure 3a), the parent ion $[Pt_2(\mu\text{-}S)_2(PPh_3)_4PbPh_3]^+$ (*m/z* 1941) dominates. Increasing the cone voltage to 80 V begins to effect fragmentation, with an ion at *m/z* 1679 being formed initially, and assigned to the species $[Pt_2(\mu\text{-}S)_2(PPh_3)_3PbPh_3]^+$, formed by dissociation of a PPh_3 ligand; at 100 V (Figure 3b) this is the base peak. Formation of another ion at *m/z* 1317 is also observed, becoming the base peak at a cone voltage of 120V (Figure 3c). This ion is assigned as the phenylated species $[Pt_2(\mu\text{-}S)_2(PPh_3)_3Ph]^+$, which may contain a μ-SPh group, and presumably formed by loss of neutral $PbPh_2$ from $[Pt_2(\mu\text{-}S)_2(PPh_3)_3PbPh_3]^+$. The parent species $[Pt_2(\mu\text{-}S)_2(PPh_3)_4Ph]^+$, which is presumably $[Pt_2(\mu\text{-}S)(\mu\text{-}SPh)(PPh_3)_4]^+$, has been generated by reaction of $[Pt_2(\mu\text{-}S)_2(PPh_3)_4]$ with phenylating agents such as PhBr and $[Ph_2I]Cl$.[15] Loss of isotopically-rich Pb has a noticeable effect in compressing the isotope envelope of the ion $[Pt_2(\mu\text{-}S)_2(PPh_3)_3Ph]^+$, compared to lead-containing ions. At 120 V, an ion at *m/z* 1055 is assigned to the species $[Pt_2(\mu\text{-}S)_2(PPh_3)_2Ph]^+$, formed by loss of an additional PPh_3 from $[Pt_2(\mu\text{-}S)_2(PPh_3)_3Ph]^+$, and at even higher voltages such as 140 V the base peak is an ion at *m/z* 977 is formed by elimination of PhH from $[Pt_2(\mu\text{-}S)_2(PPh_3)_2Ph]^+$.

Contrasting behaviour was observed in the fragmentation of the trimethyllead ion $[Pt_2(\mu\text{-}S)_2(PPh_3)_4PbMe_3]^+$ when analysed under comparable conditions; a series of spectra for **2** at increasing cone voltage are shown in Figure 4. The ion $[Pt_2(\mu\text{-}S)_2(PPh_3)_4PbMe_3]^+$ was the only major peak observed at low to moderate cone voltages (e.g. 50 V, Figure 4a). In comparable behaviour to $[Pt_2(\mu\text{-}S)_2(PPh_3)_4PbPh_3]^+$, at higher cone voltages (e.g. 90 V, Figure 4b) the first fragment ion formed was $[Pt_2(\mu\text{-}S)_2(PPh_3)_3PbMe_3]^+$ at *m/z* 1493, formed by simple loss of a PPh_3 ligand. At this cone voltage, an ion at *m/z* 1463 was also observed; this ion became the base peak at 120 V, Figure 4c. The loss of 30 Da clearly indicates fragmentation by loss of ethane, and the ion at *m/z* 1463 is assigned to $[Pt_2(\mu\text{-}S)_2(PPh_3)_3PbMe]^+$. This is similar to the fragmentation process for $[Me_3Pb]^+$ itself,[26] and analogous loss of ethane from cationic dimethyl derivatives of gold(III) and thallium(III) has been previously reported.[30] It is at this point that the fragmentation pathways of $[Pt_2(\mu\text{-}S)_2(PPh_3)_3PbMe_3]^+$ and $[Pt_2(\mu\text{-}S)_2(PPh_3)_3PbPh_3]^+$ have clearly diverged. When the cone voltage is further increased to 140 V (Figure 4d), the base peak now becomes an ion at *m/z* 1185. Examination of the high resolution isotope pattern shows that this ion has the formula $[Pt_2(\mu\text{-}S)_2(PPh_3)_2Pb\text{-}H]^+$, formed by loss of CH_4 and PPh_3 from $[Pt_2(\mu\text{-}S)_2(PPh_3)_3PbMe]^+$; this ion may contain a cyclometallated PPh_3 ligand.

Interestingly, a single crystal of $[Pt_2(\mu\text{-}S)_2(PPh_3)_4PbMe_3]PF_6$ (obtained by slow crystallisation from CH_2Cl_2-Et_2O) showed, in addition to the dominant parent ion at *m/z* 1755, a low intensity ion at *m/z* 1503, assigned as $[Pt_2(\mu\text{-}S)_2(PPh_3)_4H]^+$. A likely explanation of this is that the free sulfide centre can be protonated, destabilising the complex, resulting in the extrusion of Me_3Pb^+ and formation of the protonated species

$[Pt_2(\mu\text{-}S)_2(PPh_3)_4H]^+$. The monodentate nature of the $\{Pt_2S_2\}$ metalloligand towards the $PbMe_3^+$ fragment could promotes such a process, compared to a bidentate system (as in the $PbPh_2I^+$ derivative).

Exchange reactions have also been explored using ESI MS. Methanolic solutions of $[Pt_2(\mu\text{-}S)_2(PPh_3)_3PbMe_3]^+$ with added Ph_3PbCl, and of $[Pt_2(\mu\text{-}S)_2(PPh_3)_3PbPh_3]^+$ with added Me_3PbOAc were prepared, and analysed by ESI MS. In the former system complete exchange of the organolead groups occurred, yielding $[Pt_2(\mu\text{-}S)_2(PPh_3)_3PbPh_3]^+$, but no reaction was observed for the latter system.

Discussion

The metalloligand $[Pt_2(\mu\text{-}S)_2(PPh_3)_4]$ readily forms adducts with chemically soft lead(IV) species by displacement of halide ligands, analogous to the organo-tin(IV) systems.[6] The mode of binding of a PbR_3^+ fragment to the $\{Pt_2S_2\}$ metalloligand core appears to depend on the Lewis acidity of the lead moiety. A study of the variation in $^1J(PtP)$ coupling constants in a series of organotin(IV) adducts of $[Pt_2S_2(PPh_3)_4]$ found that the stronger Lewis acids result in observation of higher $^1J(PtP)$ values, due to their electron-withdrawing effect strengthening the Pt-P bonds.[6] In this work, the values of $^1J(PtP)$ for the lead(IV) adducts [$PbPh_2Br$ (3087 Hz) > $PbPh_2I$ (3068 Hz) > $PbPh_3$ (3013 Hz) > $PbMe_3$ (2944 Hz)] follow the expected trend and confirm that the $PbMe_3$ group is the weakest Lewis acid. For the weaker Lewis acids $PbMe_3^+$ and $PbEt_3^+$ the electronic requirements of the lead atom are readily satisfied by coordination to a single sulfide

donor, while for the stronger Lewis acid $PbPh_2I^+$, both sulfides are coordinated (one more strongly than the other in the solid state), giving a five-coordinate lead centre.

It is noteworthy that alkylation reactions occur for $[Pt_2(\mu\text{-}S)_2(PPh_3)_3PbMe_3]^+$, (through Pb-C bond cleavage) and more rapidly for $[Pt_2(\mu\text{-}S)_2(PPh_3)_3PbEt_3]^+$, but arylation does not occur at all for $[Pt_2(\mu\text{-}S)_2(PPh_3)_3PbPh_3]^+$ nor for $[Pt_2(\mu\text{-}S)_2(PPh_3)_3PbPh_2I]^+$. Although the structure of $PbPh_3^+$ adduct has not been determined, it would not be unreasonable to suggest that it has an analogous structure to the $PbPh_2I^+$ adduct, with a five-coordinate lead. Increased steric bulk at Pb and the lack of availability of a free sulfide could account for the lack of arylation reactivity in the $PbPh_3$ and Ph_2PbX (X = Br, I) systems. ESI MS observations indicate that Ph_3Pb^+ forms a more stable solution adduct with the $\{Pt_2S_2\}$ metalloligand than does Me_3Pb^+, consistent with stronger bonding to the more strongly Lewis acidic $PbPh_3^+$ fragment, which interacts with both sulfur donors.

A possible mechanism that accounts for the alkylation process is shown in Scheme 1, and involves intramolecular attack of the free sulfide group at a Pb-CH_2 carbon, resulting in transfer of the alkyl group from Pb to S. Presumably, PbR_2 is generated in this process. Simple divalent organolead compounds are known to be unstable with respect to lead(IV),[31] and PbR_2 would not be expected to be detected in the ESI mass spectrum due to the anticipated lack of an ionisation pathway. To account for the greater reactivity in the ethyl system, it is possible that the lead centre would be more electron-rich than in the methyl case (due to the positive inductive effect of the additional Me groups), so that the Pb-S bond is further weakened, the $PbEt_3^+$ group is a poorer Lewis acid still, and alkyl transfer occurs more rapidly. The observation that a key mass

spectrometric fragmentation of $[Pt_2(\mu\text{-}S)_2(PPh_3)_3PbMe_3]^+$ is *via* elimination of Me-Me, but analogous loss of Ph-Ph is not observed for $[Pt_2(\mu\text{-}S)_2(PPh_3)_3PbPh_3]^+$ is also consistent with the presence of weaker Pb-C(alkyl) bonds.

Experimental

General experimental procedures were as described in recent publications from these laboratories.[1-4] ESI mass spectra were recorded on a VG Platform II instrument in positive-ion mode, using methanol as the mobile phase. Reaction solution aliquots were diluted with methanol prior to analysis, while isolated salts were dissolved in several drops of CH_2Cl_2 before diluting with MeOH to give a total solid concentration of *ca*. 0.1 mg mL^{-1}. Confirmation of species was facilitated by comparison of observed and calculated isotope distribution patterns, the latter obtained from the *Isotope* program.[32] Reported *m/z* values are for the most intense peak in the isotope distribution envelope. Elemental analyses were obtained by the Campbell Microanalytical Laboratory at the University of Otago, Dunedin, New Zealand.

The compounds triphenyllead chloride (Aldrich), trimethyllead acetate (Aldrich), triethyllead acetate (Aldrich), tetraphenyllead (Aldrich), hexaphenyldilead (Aldrich), sodium tetraphenylborate (BDH), potassium thiocyanate (BDH), $Li[N(SO_2C_2F_5)_2]$ (3M) and ammonium hexafluorophosphate (Aldrich) were used as received. The compound $[Pt_2(\mu\text{-}S)_2(PPh_3)_4]$ was prepared by the literature procedure.[13] Diphenyllead diiodide and diphenyllead dibromide were prepared by the dropwise addition of a chloroform solution of either iodine or bromine (2 mole equiv.) to a chloroform solution of Ph_4Pb. The

product was isolated by reduction in the volume of the solution and addition of petroleum spirits, giving yellow (Ph_2PbI_2) or white (Ph_2PbBr_2) microcrystals.

Synthesis of $[Pt_2(\mu\text{-}S)_2(PPh_3)_4PbPh_3]PF_6$ 1a

A suspension of $[Pt_2(\mu\text{-}S)_2(PPh_3)_4]$ (200 mg, 0.133 mmol) and Ph_3PbCl (71 mg, 0.150 mmol) in methanol (30 mL) was stirred at room temperature, resulting in the rapid formation of a clear, bright yellow solution. After stirring for 24 h, the solution was filtered to remove a trace of insoluble matter, and to the filtrate was added NH_4PF_6 (100 mg, 0.613 mmol), resulting in the formation of a yellow microcrystalline solid. After stirring for 10 min. water (10 mL) was added to complete precipitation. The product was isolated by filtration, washed with water (10 mL) and dried under vacuum to give **1a** (198 mg, 71%) as a bright yellow solid. M.p. decomp. > 300 ºC. Found: C, 51.6; H, 3.6. $C_{90}H_{75}F_6P_5PbPt_2S_2$ requires C, 51.8; H, 3.6%. $^{31}P\text{-}\{^1H\}$ NMR, δ 21.8 [s, $^1J(PtP)$ 3013]. ESI MS *m/z* 1941, $[Pt_2(\mu\text{-}S)_2(PPh_3)_4PbPh_3]^+$ (100%).

Synthesis of $[Pt_2(\mu\text{-}S)_2(PPh_3)_4PbPh_3]BPh_4$ 1b

Following the synthesis of **1a**, complex **1b** was prepared analogously, replacing NH_4PF_6 by $NaBPh_4$ (150 mg, 0.439 mmol), resulting in the immediate formation of a light yellow precipitate; no water was added in this case. Following filtration and washing with cold methanol, complex **1b** was obtained (201 mg, 67%). Found: C, 60.3; H, 4.5. $C_{114}H_{95}BP_4PbPt_2S_2$ requires C, 60.6; H, 4.2%.

Synthesis of $[Pt_2(\mu\text{-}S)_2(PPh_3)_4PbPh_3]N(SO_2C_2F_5)_2$ 1c

Following the general procedure for **1a**, **1c** was isolated in 52% yield by addition of $LiN(SO_2C_2F_5)_2$ to the filtered reaction solution, and was obtained as small orange-yellow crystals. The presence of the cation and anion were confirmed by positive- and negative-ion [$N(SO_2C_2F_5)_2^-$, *m/z* 380] ESI MS respectively.

Synthesis of $[Pt_2(\mu\text{-}S)_2(PPh_3)_4PbPh_3]PF_6$ 1a from Pb_2Ph_6

A suspension of $[Pt_2(\mu\text{-}S)_2(PPh_3)_4]$ (200 mg, 0.133 mmol) and Pb_2Ph_6 (59 mg, 0.067 mmol) in methanol (30 mL) was stirred at room temperature, giving a clear, bright yellow solution after several hours. ESI MS showed predominantly the $[Pt_2(\mu\text{-}S)_2(PPh_3)_4PbPh_3]^+$ cation. After stirring for 36 h, the solution was filtered, and NH_4PF_6 (100 mg, 0.613 excess) added to the stirred filtrate, giving a yellow precipitate. After addition of water (30 mL), the product was filtered off, washed with water (10 mL), and dried under vacuum to give **1a** (215 mg, 77%), which was spectroscopically identical to the sample of **1a** prepared from Ph_3PbCl.

Synthesis of $[Pt_2(\mu\text{-}S)_2(PPh_3)_4PbMe_3]PF_6$ 2

Following the general method for **1a** (from Ph_3PbCl), a suspension of $[Pt_2(\mu\text{-}S)_2(PPh_3)_4]$ (200 mg, 0.133 mmol) with Me_3PbOAc (73 mg, 0.234 mmol) in methanol (30 mL) was stirred at room temperature, rapidly giving a bright yellow solution which was stirred for 1.5 h. Filtration, followed by addition of NH_4PF_6 (100 mg, 0.613 mmol) to the filtrate gave a bright yellow microcrystalline solid (199 mg, 79%). Found: C, 47.6; H, 3.8. $C_{75}H_{69}F_6P_5PbPt_2S_2$ requires C, 47.4; H, 3.7%. ESI MS *m/z* 1755, $[Pt_2(\mu\text{-}$

$S)_2(PPh_3)_4PbMe_3]^+$ (100%). $^{31}P-\{^1H\}$ NMR, δ 23.2 [s, $^1J(PtP)$ 2944]. ^1H NMR, 1.16 [s, Pb-Me, $^2J(^{207}PbH)$ 61.5] and 7.35-7.05 (m, Ph). Recrystallisation by vapour diffusion of diethyl ether into a dichloromethane solution gave bright yellow blocks.

When this reaction was repeated using a longer reaction time (>24 h), ESI MS of the isolated product, which had a slightly oily consistency, showed the presence of a substantial quantity of $[Pt_2(\mu\text{-}S)(\mu\text{-}SMe)(PPh_3)_4]^+$ at *m/z* 1518.

Synthesis of crude $[Pt_2(\mu\text{-}S)(\mu\text{-}SMe)(PPh_3)_4]PF_6$ using Me_3PbOAc

A mixture of $[Pt_2(\mu\text{-}S)_2(PPh_3)_4]$ (100 mg, 0.067 mmol) with Me_3PbOAc (36 mg, 0.116 mmol) in methanol (30 mL) was stirred, while being monitored periodically by positive-ion ESI MS. After 9 days, the dominant species observed was $[Pt_2(\mu\text{-}S)(\mu\text{-}SMe)(PPh_3)_4]^+$ at *m/z* 1518. The resulting light yellow solution was filtered to remove a trace of insoluble matter, and to the filtrate was added NH_4PF_6 (150 mg, 0.920 mmol), giving a light yellow precipitate. Water (10 mL) was added to assist precipitation, and the solid was filtered off, washed with 10 mL water, and dried under vacuum to give crude $[Pt_2(\mu\text{-}S)(\mu\text{-}SMe)(PPh_3)_4]PF_6$ (62 mg).

Synthesis of $[Pt_2(\mu\text{-}S)_2(PPh_3)_4PbPh_2I]PF_6$ 3

A suspension of $[Pt_2(\mu\text{-}S)_2(PPh_3)_4]$ (200 mg, 0.133 mmol) and Ph_2PbI_2 (110 mg, 0.179 mmol) in methanol (30 mL) was stirred at room temperature, giving a clear orange solution after *ca.* 10 minutes. A positive-ion ESI mass spectrum showed $[Pt_2(\mu\text{-}S)_2(PPh_3)_4PbPh_2I]^+$ as the dominant species. After filtration, solid NH_4PF_6 (200 mg, 1.227 mmol) was added to the filtrate, giving an orange solid, which was filtered off,

washed with water, and dried to give **3** (198 mg, 70%). Found: C, 47.2; H, 3.5. $C_{84}H_{70}F_6IP_5PbPt_2S_2$ requires C, 47.2; H, 3.3%. A positive-ion ESI mass spectrum in methanol showed a mixture of $[Pt_2(\mu\text{-}S)_2(PPh_3)_4PbPh_2I]^+$ (*m/z* 1991) and $[Pt_2(\mu\text{-}S)_2(PPh_3)_4PbPh_2]^{2+}$ (*m/z* 932). $^{31}P\text{-}\{^1H\}$ NMR, δ 16.23 [s, ^1J(PtP) 3068]. Recrystallisation by vapour diffusion of diethyl ether into a dichloromethane solution of the complex yielded bright orange crystals of **3**, shown by the X-ray structure determination to be the $.3CH_2Cl_2$ solvate. These lose solvent upon standing in air when removed from the mother liquor.

Synthesis of $[Pt_2(\mu\text{-}S)_2(PPh_3)_4PbPh_2Br]PF_6$ 4

$[Pt_2(\mu\text{-}S)_2(PPh_3)_4]$ (200 mg, 0.133 mmol) and Ph_2PbBr_2 (75 mg, 0.144 mmol) in methanol (30 mL) was stirred at room temperature for 40 min., giving a clear yellow-orange solution. After filtration, solid NH_4PF_6 (200 mg, 1.227 mmol) was added to the filtrate, giving a yellow-orange precipitate, which was filtered, washed with water, and dried to give **4** (195 mg, 70%). Found: C, 48.1; H, 3.3. $C_{84}H_{70}BrF_6P_5PbPt_2S_2$ requires C, 48.3; H, 3.4%. ESI MS: $[Pt_2(\mu\text{-}S)_2(PPh_3)_4PbPh_2Br]^+$ (*m/z* 1944, 70%) and $[Pt_2(\mu\text{-}S)_2(PPh_3)_4PbPh_2]^{2+}$ (*m/z* 932, 100%). $^{31}P\text{-}\{^1H\}$ NMR, δ 16.14 [s, ^1J(PtP) 3087].

Synthesis of $[Pt_2(\mu\text{-}S)_2(PPh_3)_4PbPh_2(SCN)]SCN$ 5

$[Pt_2(\mu\text{-}S)_2(PPh_3)_4]$ (281 mg, 0.187 mmol) and Ph_2PbBr_2 (113 mg, 0.218 mmol) in methanol (30 mL) was stirred at room temperature for 1 h. To the resulting clear yellow-orange solution was added KSCN (500 mg, large excess), resulting in the rapid deposition of a yellow precipitate. The mixture was stirred for 22 h, and the yellow

product filtered, washed with water (2 x 10 mL) and dried under vacuum to give **5** (310 mg, 84%). Found: C, 51.1; H, 3.4; N, 1.4. $C_{86}H_{70}N_2P_4PbPt_2S_4$ requires C, 52.1; H, 3.6; N, 1.4%. $^{31}P-\{^1H\}$ NMR, δ 15.73 [s, $^1J(PtP)$ 3091].

X-ray crystallography

X-ray intensity data were collected on a Bruker CCD diffractometer using standard procedures and software. Empirical absorption corrections were applied (SADABS[33]). Structures were solved by direct methods and developed and refined on F_o^2 using the SHELX programmes[34] operating under WinGX.[35] Hydrogen atoms were included in calculated positions.

Structure of $[Pt_2(\mu\text{-}S)_2(PPh_3)_4PbMe_3]PF_6$ (2)

Yellow prismatic crystals were obtained from CH_2Cl_2/Et_2O.

Crystal data: $C_{75}H_{69}F_6P_5PbPt_2S_2$, M = 1900.64, triclinic, space group P-1, *a* = 13.6472(4), *b* = 14.4319(4), *c* = 19.3433(5) Å, α = 87.624(1), β = 80.817(1), γ = 67.297(1)°, U 3468.7(2) $Å^3$, T 84(2) K, Z = 2, D_{calc} = 1.820 g cm^{-3}, μ(Mo-K_α) = 6.679 mm^{-1}, F(000) 1836; 33905 reflections collected with 2° < θ < 26°, 14132 unique (R_{int} 0.0188) used after correction for absorption ($T_{max,\ min}$ 0.281, 0.189). Crystal dimensions 0.32 x 0.28 x 0.24 mm^3.

Refinement on F_o^2 converged at R_1 0.0172 [I > 2σ (I)] and wR_2 0.0394 (all data), GoF 1.018. The structure of **2** is illustrated in Figure 1, with selected bond parameters summarised in Table 1.

Structure of $[Pt_2(\mu\text{-}S)_2(PPh_3)_4PbPh_2I]PF_6 \cdot 3CH_2Cl_2$ ($3\cdot 3CH_2Cl_2$)

Orange prismatic crystals were obtained from CH_2Cl_2/Et_2O.

Crystal data: $C_{87}H_{76}Cl_6F_6IP_5PbPt_2S_2$, M = 2391.42, triclinic, space group P-1, *a* = 12.7720(3), *b* = 17.5564(4), *c* = 19.5371(4) Å, α = 77.132(1), β = 84.108(1), γ = 86.387(1)°, U 4244.6(2) $Å^3$, T 84(2) K, Z = 2, D_{calc} = 1.871 g cm^{-3}, μ(Mo-K_α) = 6.02 mm^{-1}, F(000) 2304; 41036 reflections collected with $2° < \theta < 26°$, 17189 unique (R_{int} 0.0305) used after correction for absorption ($T_{max,\ min}$ 0.350, 0.229). Crystal dimensions 0.32 x 0.26 x 0.24 mm^3.

Refinement on F_o^2 converged at R_1 0.0466 [$I > 2\sigma$ (I)] and wR_2 0.1198 (all data), GoF 1.026. The atoms of the three solvent molecules showed relatively high U_{iso} values suggesting they were not firmly held in the lattice, and residual Δe peaks of < 5 e $Å^3$ near the I atom suggested that this also was not completely ordered. The structure of **3** is illustrated in Figure 2, with selected bond parameters summarised in Table 1.

Supplementary material

Crystallographic data (excluding structure factors) for the structures described in this paper have been deposited with the Cambridge Crystallographic Data Centre, CCDC Nos. 645598 (**2**) and 645599 (**3**). Copies of the data can be obtained free of charge on application to The Director, CCDC, 12 Union Road, Cambridge CB2 1EZ, UK (Fax: +44-1223-336033; e-mail deposit@ccdc.cam.ac.uk or www: http://www.ccdc.cam.ac.uk).

Acknowledgements

We thank the University of Waikato and the National University of Singapore (NUS) for support of this work. We also thank Kelly Kilpin for recording the NMR spectra, and Dr. Tania Groutso (University of Auckland) for collection of the X-ray data sets of **2** and **3**.

Table 1

Selected bond parameters for $[Pt_2(\mu\text{-}S)_2(PPh_3)_4PbMe_3]PF_6$ (**2**) and $[Pt_2(\mu\text{-}S)_2(PPh_3)_4PbPh_2I]PF_6$ (**3**)

	(**2**)	(**3**)
Bond lengths (Å)		
Pt(1)-S(1)	2.323(1)	2.374(2)
Pt(1)-S(2)	2.377(1)	2.351(2)
Pt(2)-S(1)	2.335(1)	2.371(2)
Pt(2)-S(2)	2.372(1)	2.362(2)
Pt-P (av)	2.292(1)	2.299(2)
Pb(1)-S(1)	3.835(1)	2.567(2)
Pb(1)-S(2)	2.611(1)	2.879(2)
Pb(1)-I(1)		2.9208(6)
Pb(1)-C(1)	2.203(3)	2.217(8)
Pb(1)-C(2)	2.209(3)	2.222(8)
Pb(1)-C(3)	2.210(3)	
Angles (º)		
P(1)-Pt(1)-P(2)	100.69(2)	97.44(7)
P(3)-Pt(2)-P(4)	103.17(2)	102.43(7)
Pt(1)-S(1)-Pt(2)	93.35(2)	86.23(6)
Pt(1)-S(2)-Pt(2)	91.06(2)	86.95(6)
Pt(1)-S(2)-Pb(1)	101.38(2)	83.42(5)
Pt(2)-S(2)-Pb(1)	99.84(2)	81.81(5)
Pt(1)-S(1)-Pb(1)		90.21(5)
Pt(2)-S(1)-Pb(1)		88.68(5)
C(1)-Pb(1)-C(2)	113.3(1)	114.4(3)
C(1)-Pb(1)-C(3)	114.3(1)	
C(2)-Pb(1)-C(3)	116.6(1)	
C(1)-Pb(1)-I(1)		96.5(2)
C(2)-Pb(1)-I(1)		99.6(2)
S(1)-Pb(1)-I(1)		89.32(4)
S(2)-Pb(1)-I(1)		156.60(4)
Dihedral angle (º)		
$P_2Pt(1)S_2/P_2Pt(2)S_2$	138.1	126.3

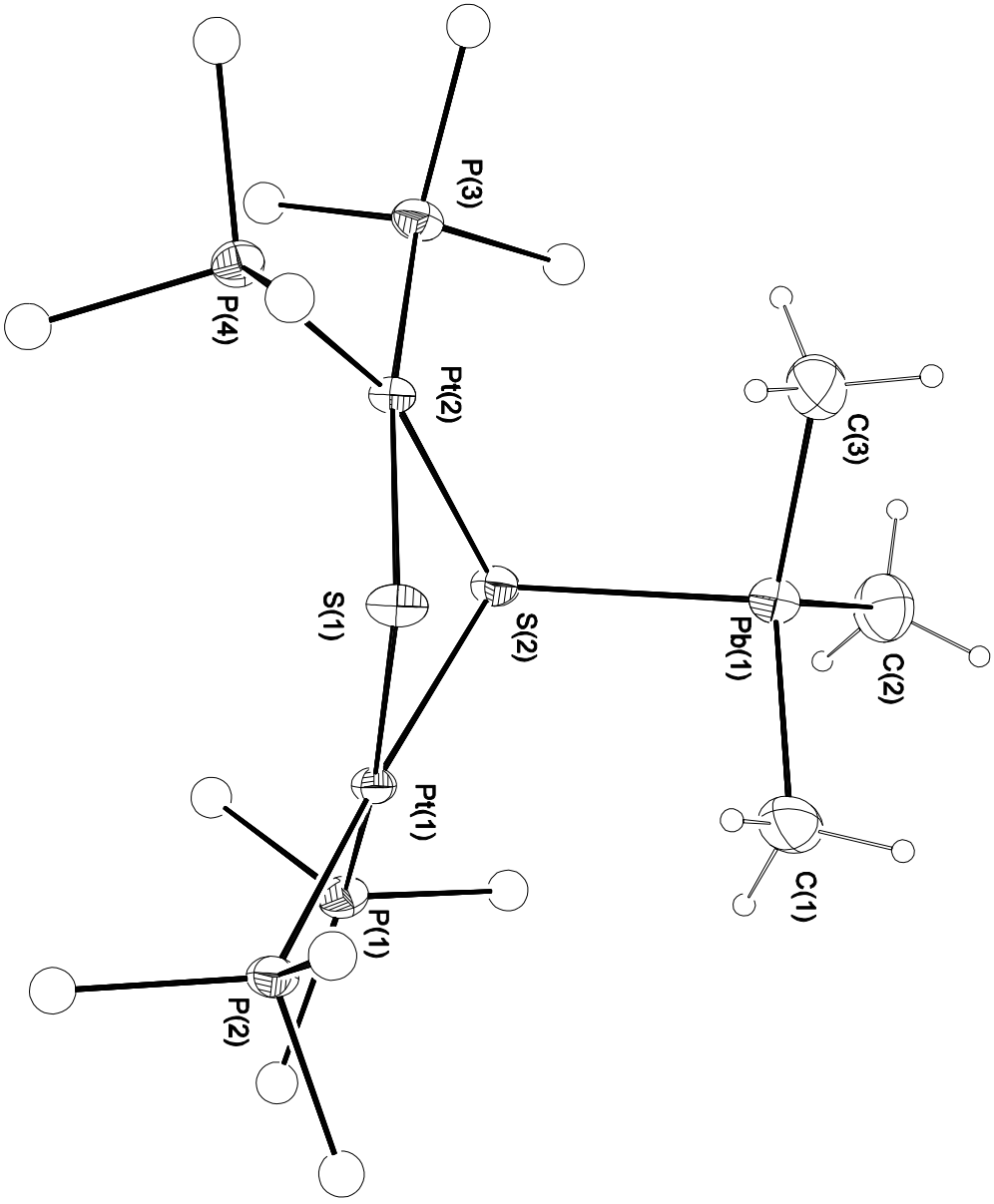

Figure 1

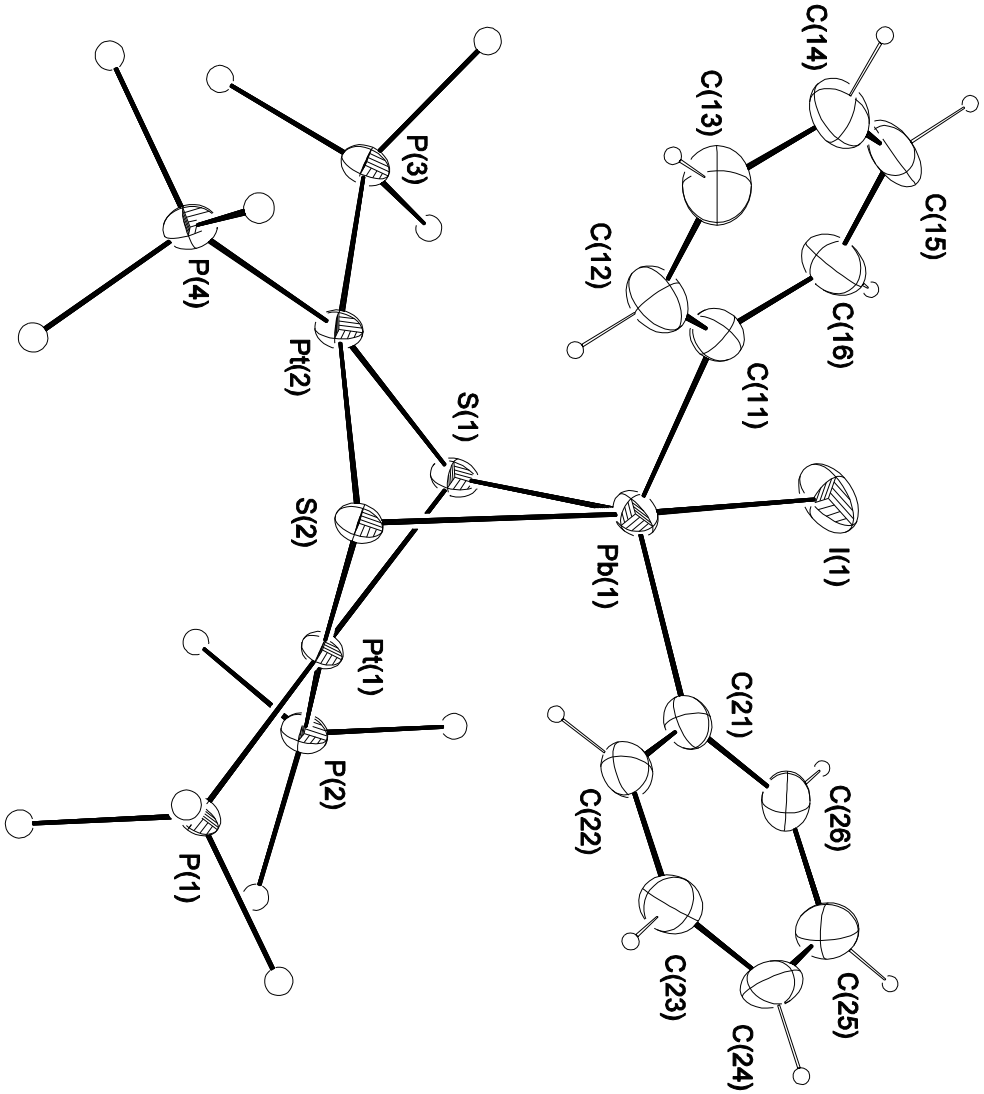
C(14)
C(13)
C(15)
C(12)
C(16)
C(11)
P(3)
P(4)
Pt(2)
S(1)
S(2)
Pb(1)
I(1)
Pt(1)
C(21)
P(2)
C(22)
C(26)
P(1)
C(23)
C(25)
C(24)

Figure 2

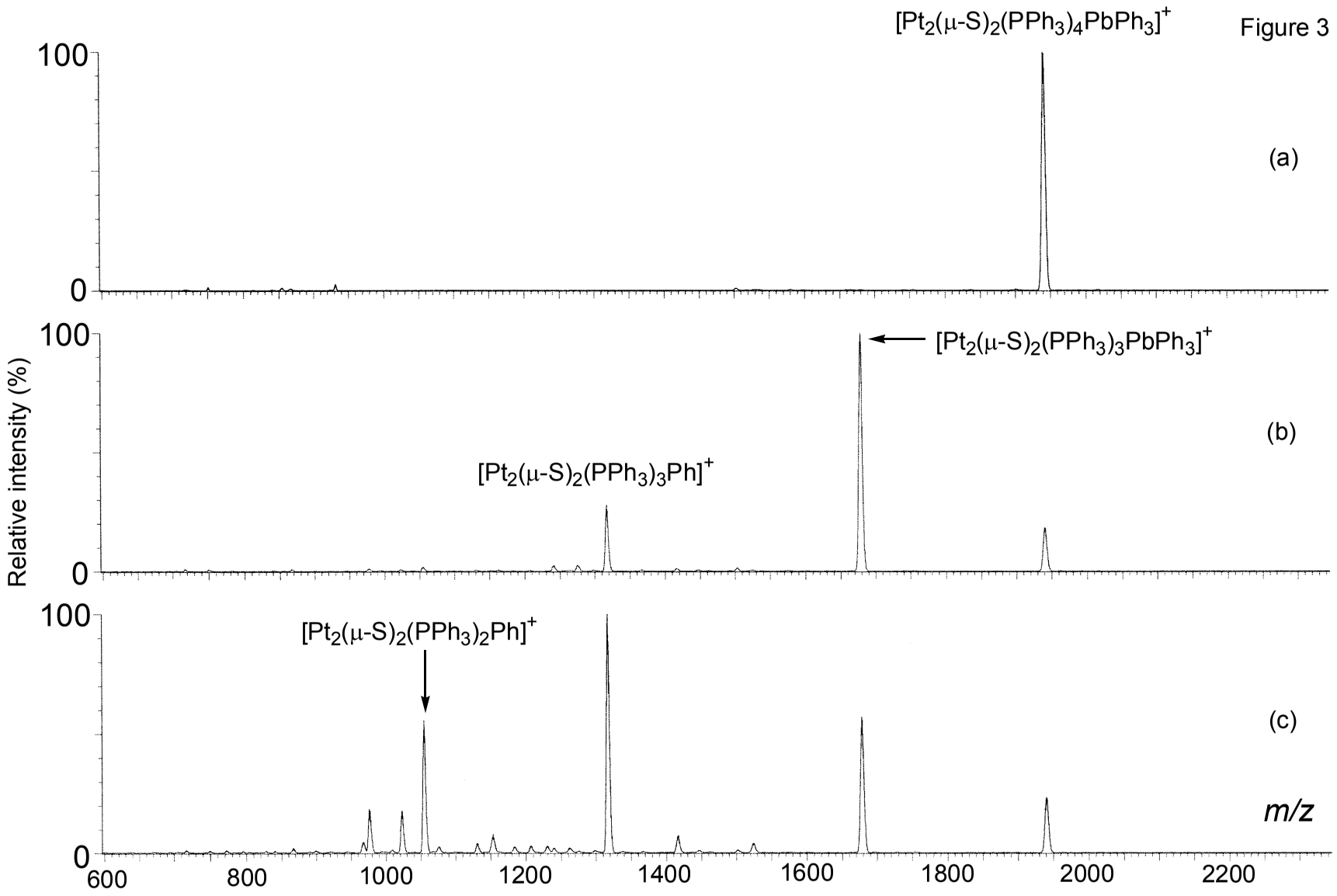
[Pt2(μ-S)2(PPh3)4PbPh3]+
Figure 3
100
0
(a)
100
[Pt2(μ-S)2(PPh3)3PbPh3]+
[Pt2(μ-S)2(PPh3)3Ph]+
(b)
0
Relative intensity (%)
100
[Pt2(μ-S)2(PPh3)2Ph]+
(c)
m/z
0
600
800
1000
1200
1400
1600
1800
2000
2200

Figure 4

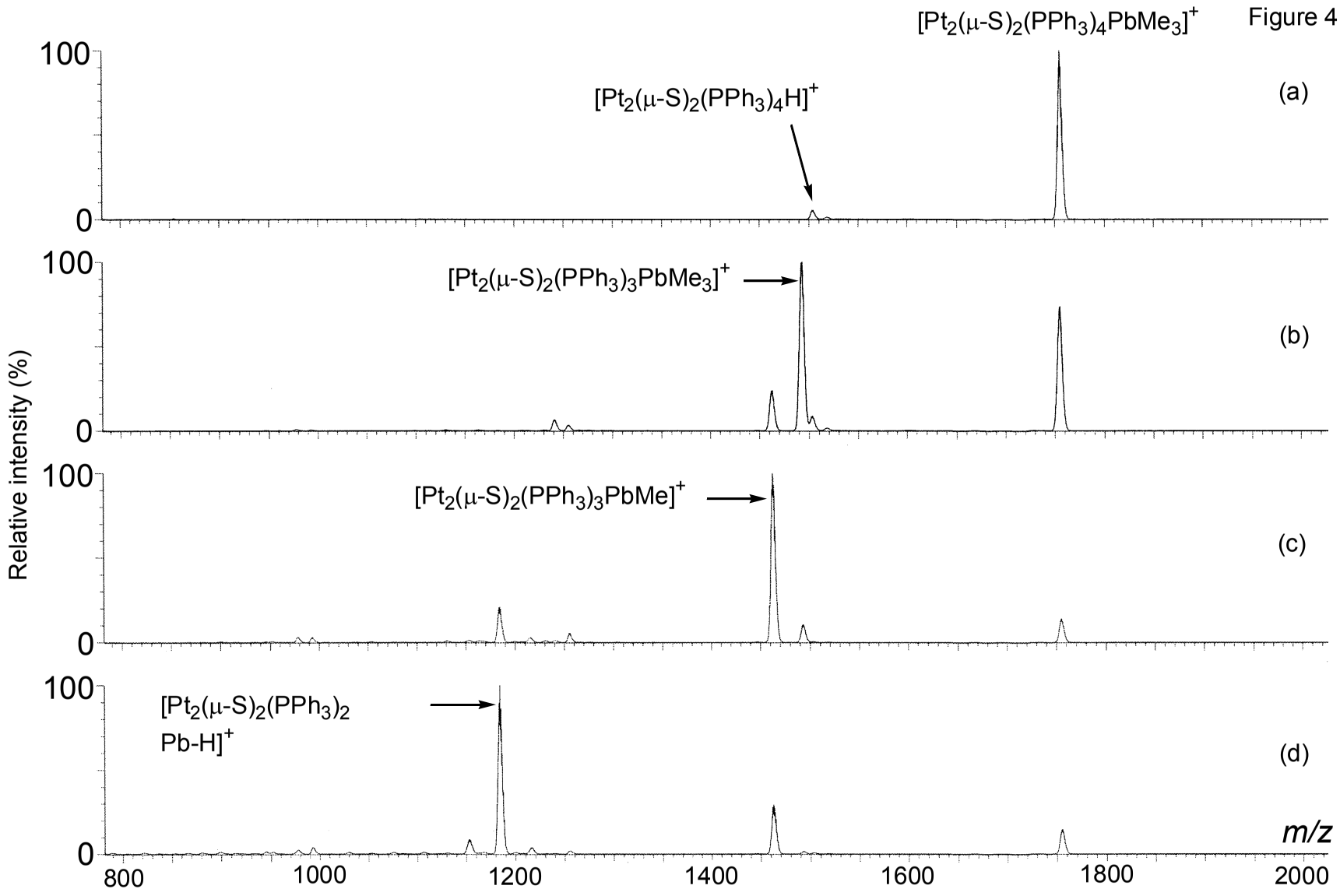
[Pt2(μ-S)2(PPh3)4PbMe3]+
[Pt2(μ-S)2(PPh3)4H]+
(a)
100
0
[Pt2(μ-S)2(PPh3)3PbMe3]+
(b)
100
0
[Pt2(μ-S)2(PPh3)3PbMe]+
(c)
100
0
[Pt2(μ-S)2(PPh3)2
Pb-H]+
(d)
100
0
Relative intensity (%)
m/z
800
1000
1200
1400
1600
1800
2000

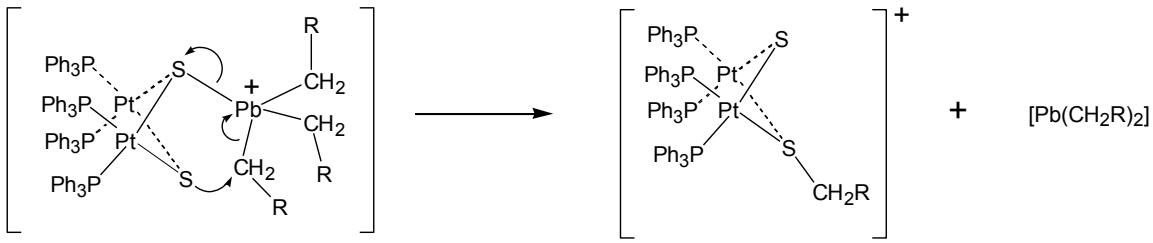

R = H or CH_3

Scheme 1

Captions for Figures

Figure 1 Structure of the cation of $[Pt_2(\mu\text{-}S)_2(PPh_3)_4PbMe_3]PF_6$ (**2**), showing the atom labelling scheme. For clarity, only the *ipso* carbon atoms of the six PPh_3 ligands have been shown.

Figure 2 Structure of the cation of $[Pt_2(\mu\text{-}S)_2(PPh_3)_4PbPh_2I]PF_6$ (**3**), showing the atom labelling scheme. For clarity, only the *ipso* carbon atoms of the six PPh_3 ligands have been shown.

Figure 3 Positive-ion ESI mass spectra of the complex $[Pt_2(\mu\text{-}S)_2(PPh_3)_4PbPh_3]PF_6$ (**1a**), at cone voltages of (a) 20V, (b) 100V and (c) 120V.

Figure 4 Positive-ion ESI mass spectra of the complex $[Pt_2(\mu\text{-}S)_2(PPh_3)_4PbMe_3]PF_6$ (**2**), at cone voltages of (a) 50V, (b) 90V, (c) 120V and (d) 140V.

References

[1] S. M. Devoy, W. Henderson, B. K. Nicholson, J. Fawcett, and T. S. A. Hor, *Dalton*, 2005, 2780.

[2] J. H. Bridson, W. Henderson, B. K. Nicholson, and T. S. A. Hor, *Inorg. Chim. Acta*, 2006, **359**, 680.

[3] S.-W. A. Fong, T. S. A. Hor, S. M. Devoy, B. A. Waugh, B. K. Nicholson, and W. Henderson, *Inorg. Chim. Acta*, 2004, **357**, 2081.

[4] S.-W. A. Fong, T. S. A. Hor, J. J. Vittal, W. Henderson and S. Cramp, *Inorg. Chim. Acta*, 2004, **357**, 1152.

[5] *Mass Spectrometry of Inorganic, Coordination and Organometallic Compounds – Tools-Techniques-Tips,* W. Henderson and J. S. McIndoe. John Wiley & Sons, 2005.

[6] S.-W. A. Fong, W. T. Yap, J. J. Vittal, T. S. A. Hor, W. Henderson, A. G. Oliver, and C. E. F. Rickard, *J. Chem. Soc., Dalton Trans*., 2001, 1986.

[7] J. S. L. Yeo, J. J. Vittal, W. Henderson, and T. S. A. Hor, *J. Chem. Soc., Dalton Trans*., 2001, 315.

[8] M. Zhou, Y. Xu, C. F. Lam, L. L. Koh, K. F. Mok, P. H. Leung and T. S. A. Hor, *Inorg. Chem*., 1993, **32**, 4660.

[9] M. Zhou, Y. Xu, A.-M. Tan, P.-H. Leung, K. F. Mok, L. L. Koh and T. S. A. Hor, *Inorg. Chem*., 1995, **34**, 6425.

[10] A. L. Tan, M. L. Chiew and T. S. A. Hor, *Theochem*, 1997, **393**, 189.

[11] F. Mirzaei, L.-B. Han and M. Tanaka, *Chem. Commun*., 2000, 657; L. C. Willemsens and G. J. M. Van Der Kirk, *J. Organomet. Chem*., 1968, **15**, 117.

[12] G. D. Shier and R. S. Drago, *J. Organomet. Chem*., 1966, **6**, 359.

[13] R. Ugo, G. La Monica, S. Cenini, A Segre and F. Conti, *J. Chem. Soc. A*, 1971, 522.

[14] C. E. Briant, C. J. Gardner, T. S. A. Hor, N. D. Howells and D. M. P. Mingos, *J. Chem. Soc., Dalton Trans.*, 1984, 2645.

[15] W. Henderson, S. H. Chong, and T. S. A. Hor, *Inorg. Chim. Acta*, 2006, **359**, 3440.

[16] C. E. Briant, G. R. Hughes, P. C. Minshall and D. M. P. Mingos, *J. Organomet. Chem*., 1980, **202**, C18.

[17] O. Schuster, A. Schier and H. Schmidbaur, *Organometallics*, 2003, **22**, 4079.

[18] A. K. Holliday and G. N. Jessop, *J. Chem. Soc. A*, 1967, 889.

[19] F. Reinholdsson, C. Briche, H. Emteborg, D. C. Baxter and W. Frech, CANAS'95 Colloquium Analytische Atomspektroskopie, 1996. CAN **126**, 176497.

[20] C. Pulham, I. Maley, S. Parsons and D. Messenger, Private Communication, 2005, Cambridge Crystallographic Database CCDC 276843.

[21] S. M. S. V. Doidge-Harrison, J. T. S. Irvine, G. M. Spencer, J. L. Wardell, P. Ganis, G. Valle and G. Tagliavini, *Polyhedron*, 1996, **15**, 1807.

[22] G. L. Wegner, R. J. F. Berger, A. Schier and H. Schmidbaur, *Z. Naturforsch*., 2000, **B55**, 995.

[23] H. O. van der Kooi, W. H. den Brinker and A. J. de Kok, *Acta Cryst*., 1985, **C41**, 869.

[24] H. Li, G. B. Carpenter and D. A Sweigart, *Organometallics*, 2000, **19**, 1823.

[25] W. Bos, J. J. Bour, P. P. J. Schlebos, P. Hageman, W. P. Bosman, J. M. M. Smits, J. A. C. van Wietmarschen and P. T. Beurskens, *Inorg. Chim. Acta*, 1986, **119**, 141; H. Liu, A. L. Tan, C. R. Cheng, K. F. Mok and T. S. A. Hor, *Inorg. Chem.,* 1997, **36**, 2916.

[26] Z. Mester and J. Pawliszyn, *Rapid Commun. Mass Spectrom.,* 1999, **13**, 1999.

[27] R. T. Aplin, J. E. H. Buston and M. G. Moloney, *J. Organomet. Chem*., 2002, **645**, 176.

[28] G. Zoorob, F. B. Brown and J. Caruso, *J. Analyt. Atom. Spectrom*., 1997, **12**, 517.

[29] J. S. Casas, M. S. Garcia-Tasende, J. Sordo, C. Taboada, M. Tubaro, P. Traldi and M. J. Vidarte, *Rapid Commun. Mass Spectrom*., 2004, **18**, 1856.

[30] A. J. Canty, R. Colton and I. M. Thomas, *J. Organomet. Chem.,* 1993, **455**, 283.

[31] I. Ahmad, Y. K. Chau, P. T. Wong, A. J. Carty and L. Taylor, *Nature*, 1980, **287**, 716

[32] L. J. Arnold, *J. Chem. Educ*., 1992, **69**, 811.

[33] R. H. Blessing, *Acta Cryst.,* 1995, **A51**, 33.

[34] G. M. Sheldrick, SHELX97 Programs for the solution and refinement of crystal structures, University of Göttingen, Germany, 1997.

[35] L. J. Farrugia, WinGX, Version 1.70.01, University of Glasgow, UK; L. J. Farrugia, *J. Appl. Cryst.,* 1999, **32**, 837.